- Radical-initiated brown carbon formation in sunlit
- carbonyl amine ammonium sulfate mixtures and

aqueous aerosol particles

4	Natalie G. Jimenez, ¹ Kyle D. Sharp, ¹ Tobin Gramyk, ¹ Duncan Z. Ugland, ¹ Matthew-Khoa Tran, ¹
5	Antonio Rojas, 1 Michael A. Rafla, 1 Devoun Stewart, 1†† Melissa M. Galloway, 1† Peng Lin, 2†††
6	Alexander Laskin, ² Mathieu Cazaunau, ³ Edouard Pangui, ³ Jean-François Doussin, ³ David O.
7	De Haan,¹*
8	
9 10	1: Department of Chemistry and Biochemistry, University of San Diego, 5998 Alcala Park, San Diego CA 92117 USA
11 12 13	2: Environmental Molecular Sciences Laboratory, Pacific Northwest National Laboratory, Richland, Washington 99352, USA, and Department of Chemistry, Purdue University, West Lafayette IN 47907 USA
14 15 16	3: Laboratoire Interuniversitaire des Systèmes Atmosphériques (LISA), UMR7583, CNRS, Université Paris-Est Créteil (UPEC) et Université de Paris, Institut Pierre Simon Laplace (IPSL), 94000 Créteil, France
17	†: now at Department of Chemistry, Lafayette College, Easton PA 18042 USA
18 19	††: now at Department of Chemistry, Sacramento City College, 3835 Freeport Blvd. Sacramento, CA 95822 USA
20 21 22	†††: now at Chemical Analysis & Emission Research Branch / ECARS, California Air Resources Board, 9528 Telstar Ave., El Monte, CA, 91713 USA
23	* Corresponding author: ddehaan@sandiego.edu, (619) 260-6882, (619) 260-2211 fax

ABSTRACT: Brown carbon (BrC) formed from glyoxal+ammonium sulfate (AS) and methylglyoxal+AS reactions photobleaches quickly, leading to the assumption that BrC formed overnight by Maillard reactions will be rapidly destroyed at sunrise. Here we tested this assumption by reacting glyoxal, methylglyoxal, glycolaldehyde or hydroxyacetone in aqueous mixtures with reduced nitrogen species at pH 4-5 in the dark and in sunlight (>350 nm) for at least 10 h. The absorption of fresh carbonyl+AS mixtures decreased when exposed to sunlight, and no BrC formed, as expected from previous work. However, the addition of amines (either methylamine or glycine) allowed BrC to form in sunlight at comparable rates as in the dark. Hydroxyacetone+amine+AS aqueous mixtures generally browned faster in sunlight than in the dark, especially in the presence of HOOH, indicating a radical-initiated BrC formation mechanism is involved. In experiments with airborne aqueous aerosol containing AS, methylamine, and glyoxal or methylglyoxal, browning was further enhanced, especially in sunlight (>300 nm), forming aerosol with optical properties similar to "very weak" atmospheric BrC. LC-ESI-MS analysis of aerosol filter extracts indicates that exposure of methylglyoxal+AS aqueous aerosol to methylamine gas, sunlight, and cloud processing increases incorporation of ammonia, methylamine, and photolytic species (e.g. acetyl radicals) into conjugated oligomer products. These results suggest that when amines are present, photolysis of 1st-generation, "dark reaction" BrC (imines and imidazoles) initiates faster, radical-initiated browning processes that may successfully compete with photobleaching, are enhanced in aqueous aerosol particles relative to bulk liquid solutions, and can produce BrC consistent with atmospheric observations.

44

45

24

25

26

27

28

29

30

31

32

33

34

35

36

37

38

39

40

41

42

- **Keywords:** secondary brown carbon, photosensitization, photobrowning, aqueous SOA,
- 46 oligomerization, aldehydes

Introduction

47

48

49

50

51

52

53

54

55

56

57

58

59

60

61

62

63

64

65

66

67

68

69

Aerosol particles negatively impact human health, 1-8 and aerosol particles that absorb light, such as brown carbon (BrC), also exacerbate climate change.⁹⁻¹⁸ Determining ways to limit atmospheric BrC concentrations is desirable on both accounts. While a majority of brown carbon is emitted directly from incomplete combustion (primary BrC), about a third is formed in the atmosphere via poorly-characterized reactions in the gas or aqueous phase. 19, 20 Significant amounts of secondary BrC are thought to be formed by aqueous Maillard reactions involving closed-shell reactions of small, water-soluble carbonyl species with ammonium or amine salts, ²¹-²⁸ producing imine intermediates²⁹ which oligomerize to form light-absorbing species (the "imine pathway"), 30-34 and by aqueous photo-oxidation of phenolic species, 35-41 especially when catalyzed by Fe(III) ions. 42-44 Co-oxidation of glyoxal and dissolved SO₂ has also been recently shown to form BrC. 45 The relative importance of these various BrC formation pathways in the atmosphere has not been determined. BrC in the atmosphere is subject to aging processes which are even less understood than BrC formation. 46-52 Light-absorbing molecules may be destroyed by hydroxyl radicals or other oxidant species that diffuse into the aqueous phase or are formed in situ.⁴⁹ Photobleaching of BrC may also occur, triggered by direct light absorption^{27, 44, 46} or indirectly via reaction with "photosensitizer" species. 53-55 Rapid photobleaching of BrC formed in mixtures of glyoxal or methylglyoxal with AS has been observed in several studies performed in bulk-phase solution. 56-⁶⁰ In some more complex systems, photolysis, photooxidation, or oxidation by radical species can at least temporarily increase BrC formation, 55, 58, 61, 62 especially in evaporating droplets. 33 In the vast majority of these studies, BrC is formed in the dark, then photolyzed or photooxidized separately, simulating a diurnal cycle, guided by an implicit assumption that BrC forms at night and is destroyed during the day. This two-step experimental design, however, does not address the extent to which BrC might form in the sunlit atmosphere, perhaps aided by radical-initiated reactions. Experimental photobleaching results are also dependent on photolysis wavelengths, highlighting the importance of simulating the solar spectrum in laboratory simulations of photobleaching.

In this work, we study the effects of sunlight and an OH radical source (hydrogen peroxide, HOOH) on aqueous-phase BrC formation involving reactions of glyoxal (GX), methylglyoxal (MG), hydroxyacetone (HA), and glycolaldehyde (GAld) with ammonium sulfate, glycine, and methylamine in order to determine whether daytime radical-initiated mechanisms play a significant role.

Methods

Bulk-phase studies. The initial UV/vis absorption spectra of bulk phase aqueous reaction mixtures (0.25 M of each reactant, pH set to 4 with oxalic or sulfuric acid) were recorded with 2 nm spectral resolution over the range 200-800 nm using 1 cm quartz cuvettes in a diode array absorption spectrometer (HP8452A). Each reaction mixture was then placed in a capped Pyrex vial with a 50% transmittance cutoff of ~350 nm, and the set of vials were exposed to ambient midday sunlight for 4 h (~12-4 pm on days with little or no cloud coverage in San Diego, California, day-to-day solar intensity varied by ~30%). A matching set of solutions were placed in most experiments at the same location under aluminum foil so that they would react in the dark at comparable temperatures. Temperature monitoring of select vials indicated that dark and sunlit samples remained within 3 °C of each other, unless specified otherwise. After the 4-h reaction time, the UV/vis spectra of the contents of each vial were recorded and the samples were stored in

the dark at 4 °C until the next day. The process was repeated for at least two subsequent days for each vial. Minimal spectral changes were observed during overnight cold storage. The initially measured absorption spectrum for each mixture was subtracted from subsequently measured spectra to generate ΔAbs difference spectra, to show the change in absorption during sample aging. Absorption changes were converted to mass absorption coefficients changes (ΔMAC) by the following equation:

$$\Delta MAC = \frac{\ln(10)\,\Delta Abs}{b\,C_{org}}$$

93

94

95

96

97

98

100

101

102

103

104

105

106

107

108

109

110

111

112

113

114

where b is the pathlength in cm and C_{org} is the sum of the concentrations of the carbonyl reactant species and the amine species (if any) in the reaction mixture in g cm⁻³. The Angstrom absorption exponents (AAE) were also characterized by power law fits to absorption spectra in the range 330 - 400 nm. This fit range was adjusted to longer wavelengths by up to 50 nm when necessary to avoid saturated absorption readings (Abs > 2.0). Aerosol studies. Mixtures of carbonyls, AS, and amines (0.056 M of each reactant) were aspirated into a 300 L Tedlar chamber. The airborne aerosol particles were then aged for 1 h in midday ambient sunlight, or indoors away from sunlight in control experiments. After 1 h of aging, aerosol particles were collected onto Teflon filters, which were then extracted in 10 mL deionized water (>18 M Ω). The absorption of filter extracts was analyzed by diode array absorption spectroscopy (HP8452A) in 1 cm cuvettes. $\triangle MAC$ values were calculated using C_{org} calculated from the mass increase of the filter during sampling divided by the extraction volume; AAE fits were determined as described above. Simulation chamber experiment / high-resolution MS analysis. 100 mM MG or 10 mM AS / 30 mM MG solutions were atomized (TSI 3076) and, for control experiments, 100 µg of diffusiondried aerosol was immediately collected onto teflon filters (Tisch, 1.0 µm pore size) without any chamber exposure time. The same AS+MG mixture was also atomized without diffusion drying into the humidified, 4.2 m³ CESAM chamber, which has been described earlier. 63, 64 There, these deliquesced seed particles were exposed to 2 ppm methylamine gas, 80 minutes of simulated sunlight, and 1-2 cloud events of 5 to 10 min. duration each, triggered by a combination of water vapor injection and a gradual, 10% pressure reduction to reach supersaturation. Chamber experimental conditions are summarized in Table S1. After processing in the chamber concluded, aerosol were collected onto Teflon filters at a flow of 15 L/min over 16 h, while chamber pressure was held constant with a compensating flow of dry nitrogen, resulting in a continuous reduction in RH during sampling. All filters were kept frozen at -20C until extraction by acetonitrile and analysis using a HPLC/PDA/HRMS platform.⁶⁵ The instrument consists of a Surveyor Plus system (including HPLC pump, autosampler and PDA detector), a standard IonMAX electrospray ionization (ESI) source, and a high resolution LTQ-Orbitrap mass spectrometer (all modules are from Thermo Electron, Inc.). Details about the experimental setup, data acquisition, peak deconvolution, and molecular formula assignment have been described previously.³² Exact masses detected for peaks with areas greater than 10⁶ and elevated relative to blank extract runs are reported here. No unexpected or unusually high safety hazards were encountered in this work.

132

133

134

135

136

137

115

116

117

118

119

120

121

122

123

124

125

126

127

128

129

130

131

Results and Discussion

<u>Carbonyl + AS mixtures.</u> Changes in absorption (expressed as ΔMAC) of aqueous mixtures containing 0.25 M carbonyl compounds and 0.25 M AS reacting for 10-14 h are shown in Figure 1. (See Figure S1 for corresponding ΔAbs graph.) Under dark conditions (green lines), the relative levels of browning observed, MG >> GX > GAld ~ HA, matches previous observations.⁶⁶ In fact,

139

140

141

142

143

144

145

146

147

148

149

150

151

152

153

154

155

156

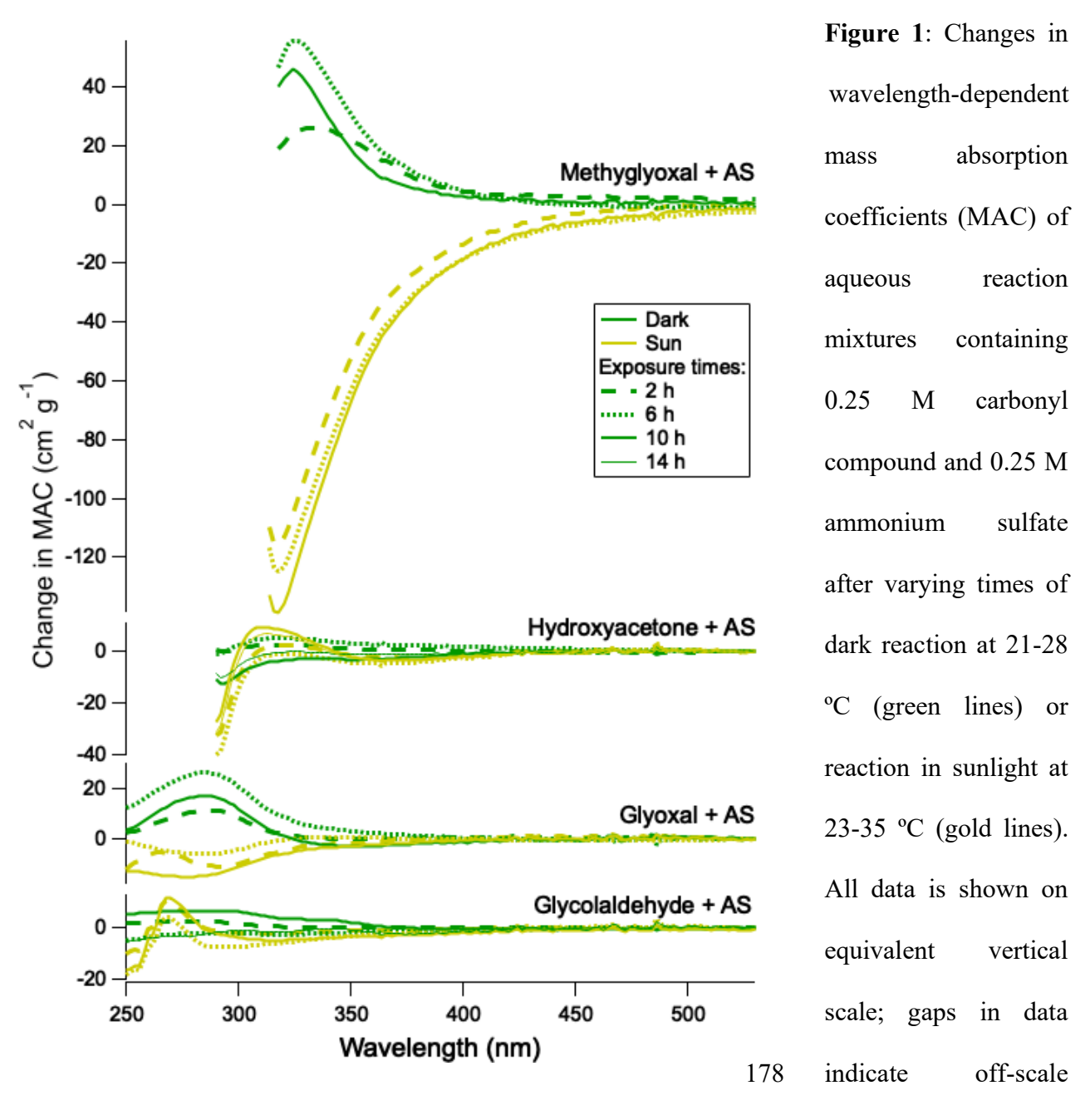
157

158

159

160

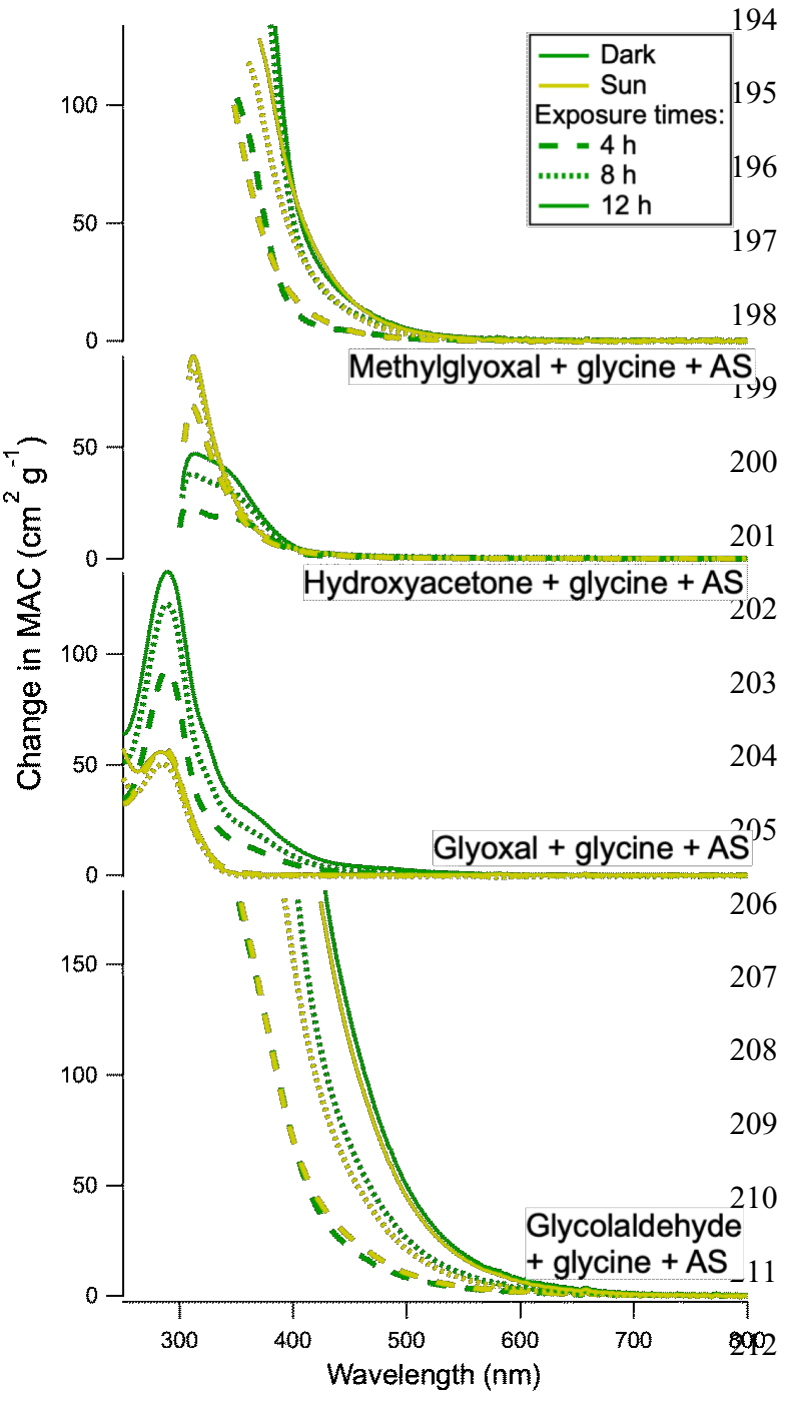
MAC increases at wavelengths below 400 nm in MG+AS and GX+AS mixtures after 6 h are quite similar to those reported after 4 days at the same pH and concentrations, 66 indicating that UVabsorbing reaction products form in these mixtures in hours rather than days under these conditions. In HA+AS and GAld+AS mixtures, however, significant browning is not observed at any wavelength even after 14 h of reaction time. Figure 1 shows that MAC increases in the visible range (> 400 nm) remains negligible (< 5 cm² g⁻¹) in all samples through 14 h of reaction time. Visible browning – the development of an absorption "tail" extending to wavelengths beyond 400 nm – is quite slow in acidified bulk aqueous samples, developing only after a few days of reaction time. 23, 25, 66 The effects of sunlight on duplicate reaction mixtures are shown in Figure 1 (gold lines). During the initial 2 h of photolysis, the overall absorption of the GX+AS and MG+AS samples declined. Clearly, no BrC is forming in sunlight, validating the conclusion of other studies that BrC formed overnight by dark GX+AS and MG+AS reactions would be rapidly destroyed during the day. 58, 59 Indeed, BrC formed by dark GX+AS and MG+AS reactions has been shown to photobleach rapidly, with a lifetime on the order of minutes, 56-59 much faster than its slow formation over hours in bulk samples, even at slightly elevated temperatures here. For GX and MG, MAC declines in sunlight in Figure 1 are strongest at wavelengths where the most browning occurred in the dark, producing \(\Delta MAC \) spectra that look like negative mirror images of those recorded under dark conditions. Declining absorption observed in sunlight indicates a loss of reactants (or loss of rapidly-formed products already present in the initial t = 0 absorption measurement) due to direct photolysis or reactions with photosensitizers. For this reason, the magnitude of these absorption losses is significantly less than what has been observed in earlier studies, where brown carbon formation was completed in a separate step before photolysis. 58, 59



absorption readings, such that *MAC* changes cannot be calculated accurately. Reaction times are indicated by line type: 2h (dashed line), 6h (dotted line), 10h (thick solid line), and 14h (thin line, GAld and HA only). Color indicates sunlit (gold) or dark (green) conditions).

For GAld+AS and HA+AS reaction mixtures (which did not brown significantly during 14 h in the dark), the effects of sunlight are subtle and wavelength-dependent. Sunlight caused the absorption of the GAld+AS sample to decrease at most wavelengths, but also caused an absorption band centered at 270 nm to appear. Similarly, sunlight caused an absorption band at 312 nm to increase in the HA+AS sample. Each of these bands increased in height by only ≤12 cm² g⁻¹ (+0.08 absorbance units) during 10 h. In contrast, absorption did not increase at any wavelength in sunlit MG+AS and GX+AS mixtures.

Carbonyl + amine + AS mixtures. It is sometimes suggested that the rapid photobleaching of MG+AS and GX+AS mixtures can be generalized to all imine-based brown carbon systems. The validity of this inference was tested in experiments where carbonyl compounds reacted with AS+glycine and AS+methylamine mixtures (Figures 2, S2, and S3).



214

Figure 2: Changes in wavelength-dependent absorption coefficients of paired aqueous reaction mixtures containing 0.25 M carbonyl compound, 0.25 M ammonium sulfate, and 0.25 M glycine after varying reaction times in sunlight (gold lines) or dark conditions (green lines). Each sun/dark sample pair was temperature-matched to within throughout reaction, MG, where except temperatures diverged by up to All data is shown on 8 °C. equivalent vertical scale; traces that do not extend to 250

nm indicate off-scale absorption readings, such that ΔMAC cannot be calculated accurately. Reaction times indicated by line type: 4 h (dashed), 8 h (thick dotted), 12 h (solid). Color indicates sunlit (gold) or dark (green) conditions). See Figure S2 for corresponding ΔAbs graphs.

217

218

219

220

221

222

223

224

225

226

227

228

229

230

231

232

233

234

235

236

237

The addition of an amine to the mixtures profoundly changes their browning behavior in the dark and especially in the sun, even though pH is held constant. In the dark, UV absorption is intensified by amine addition in all four reaction mixtures, as observed in previous studies. 66, 67 Absorption clearly extends into the visible range for GX, MG and GAld+glycine+AS solutions after a few hours reaction time. In sunlight, the presence of glycine counteracts the photobleaching of starting materials that was observed in carbonyl+AS solutions. Instead, absorption now increases under both dark and sunlit conditions for all carbonyl+glycine+AS solutions. With GX+glycine+AS, the magnitude of the absorption increase is less in sunlight than in the dark, indicating that photobleaching is occurring but cannot keep pace with BrC production. The same is true with HA+glycine+AS at wavelengths >335 nm. Browning in sunlight and in the dark is nearly identical for MG and GAld+glycine+AS solutions, suggesting that either the BrC products are resistant to photolytic degradation or that rates of photobleaching and an additional photolytically-activated browning process are nearly balanced. Generally similar browning behavior was observed using methylamine rather than glycine as the amine species (Figure S3). Methylamine-containing mixtures browned in sunlight for 12 h, but more slowly than in the dark for MG, GAld (> 340 nm), and GX+methylamine+AS (> 300 nm) reaction mixtures, which suggests that photobleaching is slower than BrC production in these systems. The extreme differences between sunlit browning in carbonyl+amine+AS mixtures and rapid photobleaching in carbonyl+AS mixtures demonstrate that the effects of sunlight on BrC formation and photobleaching cannot be generalized across imine-based BrC reaction systems. These bulkphase experiments show that carbonyls can form BrC even in the daytime atmosphere if they are present with amines in aqueous aerosol particles at high enough concentrations.

239

240

241

242

243

244

245

246

247

248

249

250

251

252

253

254

255

256

257

258

259

260

In contrast to the three aldehydes tested, the ketone species HA unexpectedly browned faster in sunlight than in the dark when mixed with AS and an amine species, especially at wavelengths below 350 nm. This indicates the existence of a fast browning mechanism initiated by a radical or photosensitizer species. This "photobrowning" was observed below 350 nm in 5 out of 8 replicate experiments on HA+methylamine+AS mixtures (Figure S4) including all three runs where methylamine was acidified with sulfuric acid. In other runs, acidifying to the same pH with oxalic acid unexpectedly⁶⁸ enhanced the dark browning of these mixtures without having a consistent effect on sunlit samples. Within each acidification group (using sulfuric or oxalic acid), while the absorption that developed in dark HA+methylamine+AS mixtures varied from experiment to experiment, likely due to day-to-day temperature variation, sunlit experiments exhibited a larger variation in absorption. This higher variation in photobrowning may be caused by the additional variable of solar intensity, and/or by an important role of some photolyticallyactive species in the mixture, such as a photosensitizer first-generation product or trace oxidant precursor absorbed from the air when the reaction vial is opened. We explore the role of one such oxidant precursor species, hydrogen peroxide, in the next section. Effects of HOOH on BrC formation. Figure 3 summarizes the effects of two different concentrations of HOOH for HA+methylamine+AS mixtures in the dark and in sunlight. In the dark, the addition of HOOH (light and dark blue lines) suppresses the buildup of light-absorbing products, especially at higher HOOH concentrations (dark blue lines), likely due to direct oxidation of BrC species. High concentrations of HOOH initially suppress the accumulation of BrC species in sunlight, too (dark red lines), but after a few hours BrC formation accelerates and eventually overtakes that of HOOH-free samples. Since HOOH is slowly being photolyzed by sunlight and converted to OH radicals, we hypothesize that the initial large excess of HOOH rapidly destroys

BrC products as they form, as seen in dark samples, while OH radicals trigger BrC production reactions that are faster than, and distinct from, the dark pathways involving only closed-shell reactants. Thus, it is only when most excess HOOH is used up that radical-initiated brown carbon products can rapidly accumulate. Furthermore, the similarity of absorption spectra in all sunlit samples after 12 h reaction times is consistent with some baseline level of OH radical production in HOOH-free samples from photosensitization by starting materials or first-generation products.⁶⁹ The hypothesis that OH catalyzes rapid brown carbon production in HA+amine+AS mixtures while excess HOOH destroys brown carbon was supported by experiments where the timing and amounts of HOOH added and the amine species were varied. With 10x less initial HOOH added (Figure 3), some suppression of browning was still observed in the dark (light blue lines), but rapid browning in sunlight (orange lines) started immediately, without the initial induction period seen with higher HOOH concentrations. In other experiments, 0.25 M HOOH was added not only at t = 0 but also at 4, 8, and 12 h (Figure S6) to test the effects of replenishing excess HOOH. In these experiments, no significant browning was observed, and some photobleaching occurred below 325 nm, further supporting the idea that excess HOOH destroys brown carbon or its precursors. Similar results were observed in experiments where methylamine was replaced with glycine (Figure S7). Although absorption increased more slowly at 350 nm with glycine, the most brown carbon still formed when solutions containing lower levels (0.025 M) of HOOH were exposed to several hours of sunlight. Clearly sunlight and especially OH radicals enhance BrC production in HA+amine+AS reaction mixtures, pointing to the importance of radical-initiated BrC formation pathways in this reaction system.

283

261

262

263

264

265

266

267

268

269

270

271

272

273

274

275

276

277

278

279

280

281

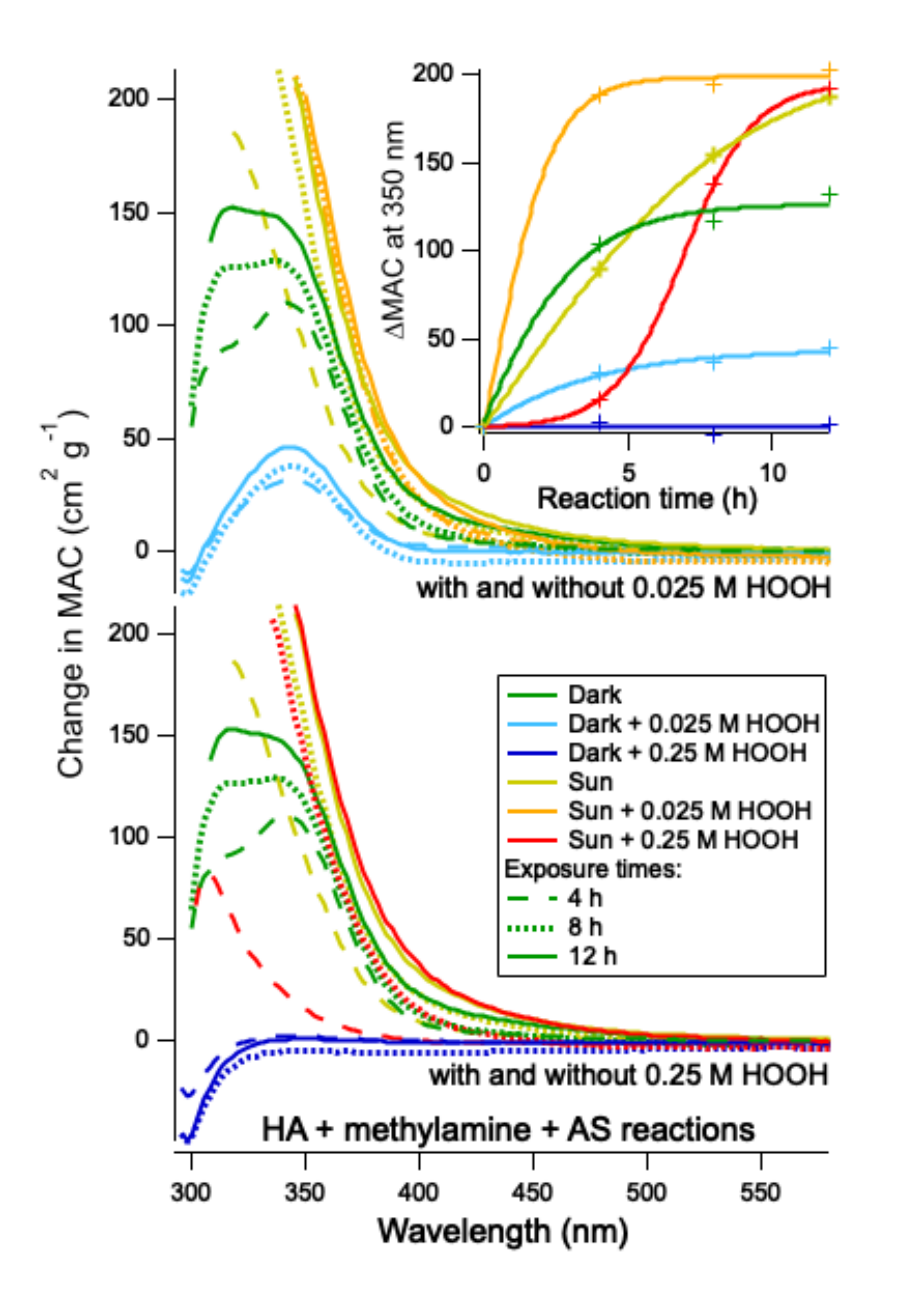


Figure 3: Changes in wavelength-dependent absorption mass coefficients of paired reaction mixtures containing 0.25 M HA, methylamine, and AS in sunlight (gold) or dark (green) after (dashed lines), (dotted lines), or 12 h (solid lines). Top panel: comparison with identical mixtures with 0.025 M HOOH in sunlight (orange) or in dark (light blue).

Lower panel: comparison with identical mixtures with 0.25 M HOOH in sunlight (red) or in dark (dark blue). Inset: ΔMAC at 350 nm vs time, using same color code. See Figure S5 for corresponding ΔAbs graphs.

304

305

306

301

302

303

<u>Carbonyl + amine + AS aerosol particles</u>. Since absorption spectra⁵¹ and browning chemistry can differ in suspended aerosol particles from that in bulk solutions,^{70, 71} aqueous aerosol particles

were generated in Tedlar bags and exposed to either in full-spectrum sunlight or ambient indoor light while suspended in air, before filtration and extraction. The mass absorption coefficients (MAC) of filter extracts from suspended aerosol experiments are summarized in Figure 4. For the GX + methylamine + AS system (top panel), aerosol-phase browning between 300 and 400 nm is more pronounced when particles are aged in sunlight rather than indoor ambient light, with or without added HOOH. This is the opposite of what is observed at these wavelengths when bulk solutions are exposed to sunlight (Figure S3, 3rd panel), demonstrating that photolytically-driven radical reactions can produce GX-derived BrC material in sunlight, not just at night, at enhanced rates in suspended aqueous aerosol particles compared to bulk liquid samples. While the addition of 1.7 mM HOOH to the aerosol-generation liquid suppressed BrC formation to some extent in both sunlight and indoor experiments, the 1 h photolysis time in these experiments may have been insufficient to eliminate excess HOOH. In any case, sunlit samples still browned more than dark samples in the presence of HOOH.

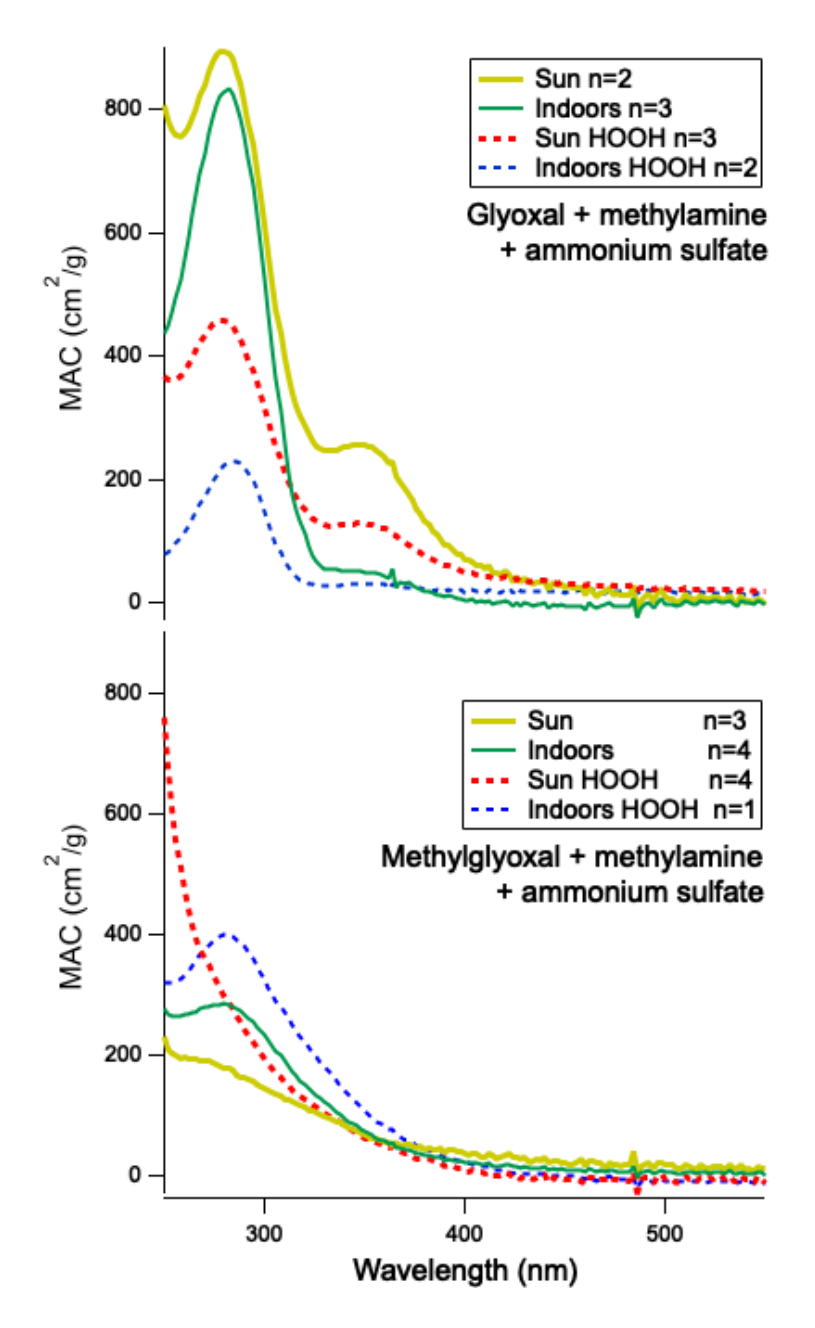


Figure 4: Wavelength-dependent mass absorption coefficients of aerosol filter extracts from small chamber experiments. Aqueous aerosol were generated from solutions containing 0.056 dicarbonyl compound, methylamine, and AS, aged for ~1 h in sunlight (gold lines) or ambient indoor light (green lines). With added 0.0017 M HOOH in sunlight (red dashes), or ambient indoor light (blue dashes). Top panel: GX. Bottom panel: MG. Numbers of experiments averaged into each line are shown in legends.

338

339

340

341

342

For MG+methylamine+AS aerosol, slightly more browning is observed in particles protected from sunlight than in those exposed to sunlight (Figure 4 bottom panel), even in the presence of HOOH, but the difference is smaller than in bulk solutions (Figure S3, 1st panel). Taken together, these results for dicarbonyl+methylamine+AS solutions suggest that photosensitization / radical-

induced browning can be enhanced in aerosol particles relative to bulk liquid solutions with the same reactants present. This is important because most BrC photobleaching studies to date have been performed on bulk liquid solutions, ⁵⁶⁻⁶⁰ even if the brown carbon was initially formed in suspended aerosol. ⁵⁹

The optical parameters of BrC from each experiment are compared to the recent atmospheric BrC classification scheme of Saleh *et al.*^{72, 73} in Figure 5. It can be seen that BrC formed in dark, bulk-phase reactions between carbonyl species and AS (black triangle) does not match atmospheric BrC in absorptivity, expressed as log(MAC₄₀₅), and on average has a wavelength dependence (expressed as AAE₃₃₀₋₄₀₀) that is steeper. (Since no BrC forms from this system in sunlight, this condition cannot appear in Figure 5.) The addition of an amine species to bulk-phase carbonyl+AS mixtures brings the wavelength dependence of absorption into the range of very weak BrC and allows brown carbon to form in the sun, but the average MAC values are still lower than atmospheric BrC. MAC values extracted from aerosol-phase experiments are higher than in bulk-phase experiments, especially in experiments where suspended aerosol were exposed to 1 h of sunlight. Under these sunlit aerosol conditions, the BrC formed from carbonyl+AS+amine reactions, on average, matched the wavelength dependence and absorptivity of the "very weak" class of BrC observed in the atmosphere. Thus, carbonyl+AS+amine reactions, but not carbonyl+AS reactions, may be an atmospheric source of this type of weakly-absorbing BrC.

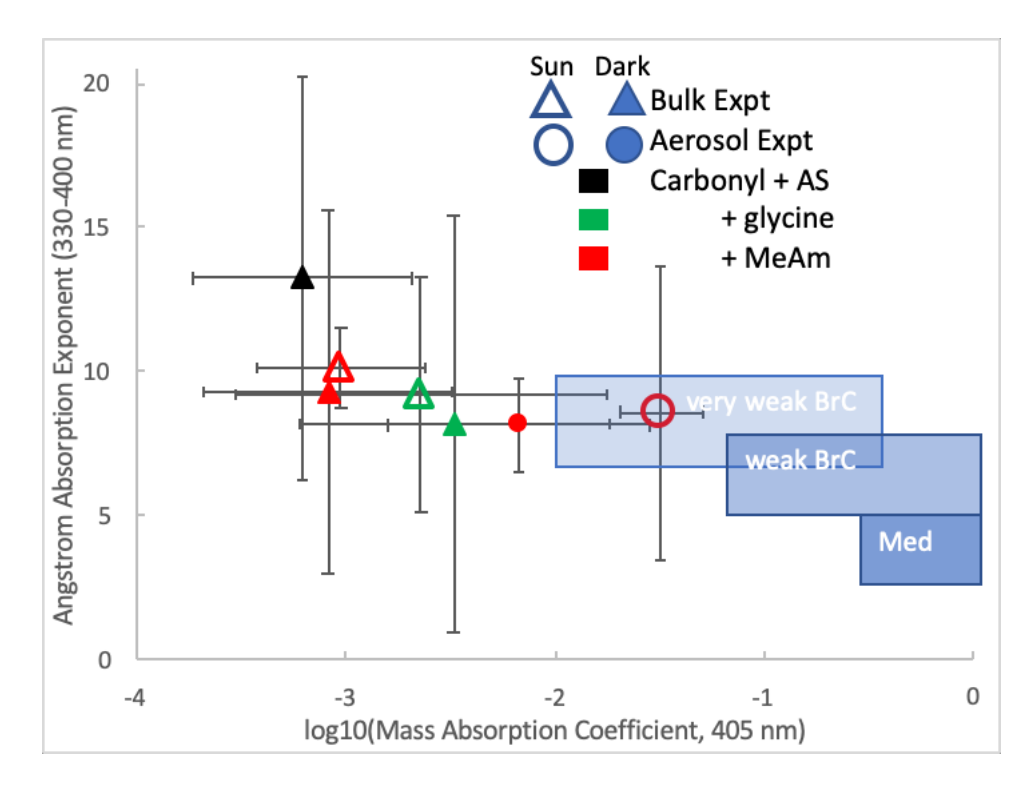


Figure 5: Optical parameters of BrC formed in this study compared to Saleh's field-based BrC classification scheme, graphed as Angstrom absorption exponent vs MAC₄₀₅. Each data point represents an average of experiments with different carbonyl compounds; shapes indicate bulk phase (triangle) or aerosol phase (round) experiments, while fill indicates dark (filled) or sunlit (open symbol) conditions. All experiments contain carbonyl species and ammonium sulfate. Symbol color indicates amine present: no amine (black), methylamine (red), or glycine (green).

Chemical analysis of aerosol particles. Additional MG+methylamine+AS experiments with offline LC-ESI-MS analysis were conducted in the CESAM chamber to further our mechanistic understanding of the photolytic browning pathway involving amines. In these experiments we compared pure MG seed aerosol particles and 3:1 MG:AS seed aerosol particles with no chamber exposure to 3:1 MG:AS aerosol particles that had been exposed to 2 ppm methylamine gas, 80 minutes of simulated sunlight, and cloud processing in the chamber. A list of observed ions with

exact masses, peak area ranking, minimum light/dark experiment peak area ratios, and proposed molecular formulae, structures, and precursor species is shown in Table 1. Product molecules detected only with chamber exposure to methylamine and sunlit clouds are labeled "unique," while remaining products are listed in order from most increased to most decreased due to chamber exposure.

Table 1: Changes in Reaction Products Detected in Methylglyoxal+AS Aerosol Particles Upon Exposure to Methylamine Gas, Simulated Sunlight, and Cloud Processing

Exptl. ion	Peak	Peak	Neutral	Ionization	Δ^{a}	Possible structure
m/z	area	area	formula		(ppm)	
	rank,	ratio vs	(precursor		41,	
	post-	seed	species)			
	exposure	particles				
311.2191	12	unique ^b	$C_{14}H_{26}N_6O_2$	H^+	1.5	O NH ₂ O NH ₂
			(4MG			N
			2MA 4NH ₃)			
						йн ни й
198.1477	13	unique ^b	C ₁₁ H ₁₉ NO ₂	$\mathrm{H}^{\scriptscriptstyle +}$	8.4	OH
		. 1	(5AAld			
			,			, , , , , , , , , , , , , , , , , , ,
			1MA)			
						l oh
217.0500	17	unique ^b	C ₁₀ H ₁₀ O ₄	Na ⁺	-10.6	0
			(3MG			
			1AAld -			
			1CO ₂)			он Ü
		. ,				NH ₂ NH NH
267.1928	19	unique ^b	$C_{12}H_{22}N_6O$	H^+	1.9	
			(3MG 1HA			OH
			6NH ₃)			
						NH NH ₂ NH
214.1188	5	3.5	C ₉ H ₁₅ N ₃ O ₃	H^+	1.8	O NH ₂ O
			(3MG			HN
			3NH ₃)			
			ŕ			O 14112

368.2410	10	2.0	C ₁₆ H ₂₉ N ₇ O ₃ (5MG 1MA 6NH ₃)	H ⁺	0.1	NH ₂ O NH ₂ NH ₂ NH ₂ NH ₂
301.1410	1	1.8	C ₁₃ H ₂₀ N ₂ O ₆ (4MG 1MA 1NH ₃)	H ⁺	-3.5	HO OH ONH2 OH
185.0420	3	0.038	C ₆ H ₁₀ O ₅ (2MG)	Na ⁺	2.9	но Он Он
140.0021	4	0.022	C ₂ H ₅ NSO ₄ (1AAld 1SO ₄ 1NH ₃)	H^{+}	-2.4	NH O OH
329.0843	7	0.012	C ₁₂ H ₁₈ O ₉ (4MG)	Na ⁺	1.6	HO OH O OH O Na ⁺
347.0950	2	0.0034	C ₁₂ H ₂₀ O ₁₀ (4MG)	Na ⁺	1.1	HO OH OH OH OH
126.0391	6	0.0024	$C_2H_4O_5$	$\mathrm{NH_4}^+$	9.0	Oxalic acid hydrate

Seven peaks detected by positive ion mode ESI-MS that increased in sunlight are listed, followed by the five largest peaks that decreased in sunlight (ratio < 1), listed in order of decreasing light-to-dark experiment peak area ratios. Molecular formulas were detected as H^+ adducts unless otherwise stated. Many of the possible structures shown could reversibly form several different heterocyclic structures via nucleophilic attack of an NH_2 or OH group on a C=O or C=N carbon. Abbreviations: MG = methylglyoxal. MA = methylamine. NH_3 = ammonia. AAld = acetaldehyde or acetyl radical. $-1CO_2$ = photolytic decarboxylation. HA = hydroxyacetone, formed from MG photolysis. SO_4 = sulfate ion. a: nominal – measured mass. b: detected only in experiments with simulated sunlight, listed in order from largest to smallest peak areas.

At the bottom of Table 1, it can be seen that major MS peaks that decreased in size after chamber exposure to methylamine and sunlit clouds (ratios < 1) all have exact masses that match species containing 0 or 1 nitrogen atom per molecule. These species include methylglyoxal dimer and

tetramer species (likely formed by aldol condensation) and a proposed imine-organosulfate species that was present only in experiments where ammonium sulfate was included in seed particles. On the other hand, peaks that increased in size during chamber exposure (Table 1 top) matched molecular formulae with 2 to 7 N / molecule. Exposure to methylamine in the chamber appears to have increased both methylamine and ammonia incorporation into aqueous-phase products, likely due to methylamine's favorable exchange reaction with dissolved ammonium salts, producing ammonia and methylaminium ions. Calculating an average number of N / molecule weighted by peak area as described in the SI, we find that chamber exposure of methylglyoxal+AS aerosol to methylamine and sunlit clouds increased the number of nitrogens per detected organic molecule from 1.0 to 2.0, dominated by the production of C₁₃H₂₀N₂O₆ (*m/z* 301.1410) and its incorporation of one methylamine and one ammonia molecule.

Unique peaks that were seen only after chamber exposure to methylamine and sunlit clouds were

Unique peaks that were seen only after chamber exposure to methylamine and sunlit clouds were assigned to proposed molecular structures containing 3-6 double bonds, and appear to form from precursors including methylamine, acetaldehyde / acetyl radicals, and/or HA. The formation of the unique $C_{10}H_{10}O_4$ m/z 217.0500 product also appears to involve oxidation followed by decarboxylation, which can be catalyzed by ammonium salts.⁷⁴ Chamber exposure increased the weighted average number of conjugated double bonds per molecule from 1.0 (non-conjugated) to 3.0, again dominated by the production of $C_{13}H_{20}N_2O_6$ (m/z 301.1410) with its four double bonds, three of which are conjugated. In summary, exposure to methylamine, sunlight, and cloud processing results in the conversion of MG oligomers into more conjugated product molecules that incorporate more nitrogen (both methylamine and ammonia) and photolysis products (acetyl radicals and HA).

419

420

421

422

423

424

425

426

427

428

429

430

431

432

433

434

435

436

437

438

439

440

While it was apparent in a recent study that acetyl radicals played a central role in the photooligomerization chemistry of methylglyoxal, ⁶⁴ the source of these radicals was unclear. Hydration of methylglyoxal, even in the gas phase, 75 removes any absorption bands in the actinic range, 76 suggesting that direct photolysis of aqueous methylglyoxal is unlikely in the atmosphere or in any realistic laboratory simulation. Aqueous solutions of HA, GX, and GAld are less light-absorbing than MG, making direct photolysis of these dissolved compounds even less likely. Once small carbonyl species react with reduced nitrogen compounds in the aqueous phase, however, imines and derivatized N-containing heterocyclic products are formed.⁷⁷ These products are more strongly light absorbing than the reactants, moving absorption into the actinic range where light absorption can occur.^{23,25} In dark reactions with GX, common atmospheric amines such as glycine and methylamine have been shown to be more effective than ammonium salts at generating C-N bonds⁶⁷ and light-absorbing products.^{66, 67} Thus, it is likely that photolysis of first-generation carbonyl + amine BrC products generate the radical species that trigger further oligomerization and brown carbon production. For example, imidazole derivatives are a class of photosensitizer C-N reaction products^{53, 78, 79} that have been detected in aqueous-phase reactions of AS with all four carbonyl compounds used in this study.⁷⁷ Replacing ammonia with primary amines in the dark chemical mechanism produces a permanently charged imidazolium ring whose absorption is red-shifted by ~10 nm compared to a neutral imidazole ring formed with ammonia. 80 Additional functional groups attached to the carbon atoms in heterocyclic rings further red-shift the absorption bands.⁷⁷ The increased overlap of such N-containing reaction products with the solar spectrum is expected to increase production of radicals and excited-state photosensitizer species in the aqueous aerosol phase. In recent AS-free studies of BrC aerosol formation by methylglyoxal+methylamine

reactions,⁶⁴ it was noted that imidazolium derivatives were formed upon exposure to methylamine gas, but then were greatly reduced or eliminated upon exposure to sunlight, suggesting that such compounds are the source of not only triplet carbon excited state species but also photolysis fragment radicals that trigger further oligomerization and browning in sunlight. This result is consistent with the MS product analysis in Table 1, where N-methyl imidazole species were not detected in aerosol after combined methylamine and sunlight exposure in the chamber.

Radical and/or excited state species, once produced, will rapidly react with nearby molecules in crowded aqueous environments, and especially at the air-water interface where surface-active molecules accumulate. This effect has been noted in bulk aqueous-phase experiments on carbonyl compounds, where oxidation by OH radicals generated oligomeric products only at high concentrations due to accretion reactions between organic radical intermediates and other organic molecules. A similar effect is evidently at work in the light-activated formation of brown carbon oligomers in the carbonyl+AS+amine aqueous reaction system. Moreover, the dominance of light-activated radical reaction pathways involving surface-active BrC may be explain the observed divergent behavior between photobleaching experiments performed in bulk solution and in suspended droplets. S1

Acknowledgments. This work was funded by NSF grants AGS-1523178 and AGS-1826593. The CESAM chamber aerosol aging experiments were part of a project that has received funding from the European Union's Horizon 2020 research and innovation program under grant agreement No 730997. CNRS-INSU is gratefully acknowledged for supporting CESAM as an open facility through the National Instrument label, as well as the AERIS data center (https://www.aerisdata.fr/) for hosting, curating, and distributing CESAM chamber data via EUROCHAMP-2020 databases. The HPLCPDA-ESI-HRMS measurements were performed on project award

(10.46936/sthm.proj.2015.48884/60005735) at the Environmental Molecular Sciences
 Laboratory, a DOE Office of Science User Facility sponsored by the Biological and Environmental
 Research program under Contract No. DE-AC05-76RL01830.

Supplemental Information: Description of calculations of peak-weighted N atoms and conjugated double bonds per detected molecule, additional absorption change graphs, MG/GX/GAld/HA+methylamine+AS experiment data, effects of acidifying samples with oxalic vs sulfuric acid, data summaries of additional HOOH addition experiments, and summary table of large chamber aerosol processing experiments.

TOC artwork



476 **References**

- 1. Schwartz, J., Air pollution and daily mortality: a review and meta analysis. *Environ. Res.* **1994**, *64*, (1), 36-52. doi:10.1006/enrs.1994.1005
- 2. Schwartz, J., What are people dying of on high air pollution days? *Environmental Research* **1994**, *64*, (1), 26-35. doi:10.1006/enrs.1994.1004
- 481 3. Kao, A. S.; Friedlander, S. K., Temporal variations of particulate air pollution: a marker for free radical dosage and adverse health effects? *Inhal. Toxicol.* **1995,** 7, (1), 149-156. doi:10.3109/08958379509014278
- 484 4. Gilmour, P. S.; Brown, D. M.; Lindsay, T. G.; Beswick, P. H.; MacNee, W.; Donaldson, K., Adverse health effects of PM10 particles: involvement of iron in generation of hydroxyl radical. *Occup Environ Med* **1996**, *53*, (12), 817-822. doi:10.1136/oem.53.12.817
- 487 5. Harrison, R. M.; Yin, J., Particulate matter in the atmosphere: which particle properties are important for its effects on health? *The Science of The Total Environment* **2000**, *249*, (1-3), 85-101. doi:10.1016/s0048-9697(99)00513-6
- 490 6. Poschl, U., Atmospheric aerosols: Composition, transformation, climate and health effects.
 491 *Angew Chem Int Edit* **2005**, *44*, (46), 7520-7540. doi:DOI 10.1002/anie.200501122
- 7. Kennedy, I. M., The health effects of combustion-generated aerosols. *Proceedings of the Combustion Institute* **2007**, 31, (2), 2757-2770. doi:https://doi.org/10.1016/j.proci.2006.08.116
- 8. Wu, S.; Deng, F.; Wei, H.; Huang, J.; Wang, X.; Hao, Y.; Zheng, C.; Qin, Y.; Lv, H.; Shima, M.; Guo, X., Association of cardiopulmonary health effects with source-appointed ambient fine particulate in Beijing, China: A combined analysis from the Healthy Volunteer Natural Relocation (HVNR) study. *Environ Sci Technol* **2014**, *48*, (6), 3438-3448. doi:10.1021/es404778w
- 9. Ramanathan, V.; Li, F.; Ramana, M. V.; Praveen, P. S.; Kim, D.; Corrigan, C. E.; Nguyen, H.; Stone, E. A.; Schauer, J. J.; Carmichael, G. R.; Adhikary, B.; Yoon, S. C., Atmospheric brown clouds: hemispherical and regional variations in long-range transport, absorption, and radiative forcing. *J. Geophys. Res.* **2007**, *112*, (D12), D22S21/1-D22S21/26. doi:10.1029/2006JD008124
- 505 10. Bahadur, R.; Praveen, P. S.; Xu, Y.; Ramanathan, V., Solar absorption by elemental and brown carbon determine from spectral observations. *Proc. Natl. Acad. Sci. (USA)* **2012,** *109*, (43), 17366-17371. doi:10.1073/pnas.1205910109
- 508 11. Feng, Y.; Ramanathan, V.; Kotamarthi, V. R., Brown carbon: a significant atmospheric absorber of solar radiation? *Atmos. Chem. Phys.* **2013**, *13*, (17), 8607-8621. doi:10.5194/acp-13-8607-2013
- 12. Laskin, A.; Laskin, J.; Nizkorodov, S. A., Chemistry of Atmospheric Brown Carbon. *Chem. Rev.* **2015**, *115*, 4335-4382. doi:10.1021/cr5006167
- 513 13. Shamjad, P. M.; Tripathi, S. N.; Pathak, R.; Hallquist, M.; Arola, A.; Bergin, M. H., Contribution of Brown Carbon to Direct Radiative Forcing over the Indo-Gangetic Plain.

 515 Environ Sci Technol 2015, 49, (17), 10474-10481. doi:10.1021/acs.est.5b03368
- 516 14. Chakrabarty, R. K.; Gyawali, M.; Yatavelli, R. L. N.; Pandey, A.; Watts, A. C.; Knue, J.; Chen, L. W. A.; Pattison, R. R.; Tsibart, A.; Samburova, V.; Moosmüller, H., Brown carbon aerosols
- from burning of boreal peatlands: microphysical properties, emission factors, and implications
- for direct radiative forcing. *Atmos. Chem. Phys.* **2016**, *16*, (5), 3033-3040. doi:10.5194/acp-16-3033-2016

- 15. Zhang, Y.; Forrister, H.; Liu, J.; Dibb, J.; Anderson, B.; Schwarz, J. P.; Perring, A. E.; Jimenez,
 J. L.; Campuzano-Jost, P.; Wang, Y.; Nenes, A.; Weber, R. J., Top-of-atmosphere radiative
 forcing affected by brown carbon in the upper troposphere. *Nature Geosci.* 2017, 10, 486-489.
 doi:10.1038/ngeo2960
- 16. Brown, H.; Liu, X.; Feng, Y.; Jiang, Y.; Wu, M.; Lu, Z.; Wu, C.; Murphy, S.; Pokhrel, R., Radiative effect and climate impacts of brown carbon with the Community Atmosphere Model (CAM5). *Atmos. Chem. Phys.* **2018**, *18*, (24), 17745-17768. doi:10.5194/acp-18-17745-2018
- 528 17. Zhang, A.; Wang, Y.; Zhang, Y.; Weber, R. J.; Song, Y.; Ke, Z.; Zou, Y., Modeling global 529 radiative effect of brown carbon: A larger heating source in the tropical free troposphere than 530 black carbon. *Atmos. Chem. Phys. Discuss.* **2019**, 2019, 1-36. doi:10.5194/acp-2019-594
- 18. Tuccella, P.; Curci, G.; Pitari, G.; Lee, S.; Jo, D. S., Direct radiative effect of absorbing aerosols: sensitivity to mixing state, brown carbon and soil dust refractive index and shape.

 Journal of Geophysical Research: Atmospheres 2020, 125, (2), e2019JD030967.

 doi:10.1029/2019JD030967
- 19. Mukai, H.; Ambe, Y., Characterization of a humic acid-like brown substance in airborne particulate matter and tentative identification of its origin. *Atmospheric Environment (1967)*1986, 20, (5), 813-819. doi:https://doi.org/10.1016/0004-6981(86)90265-9
- 20. Hecobian, A.; Zhang, X.; Zheng, M.; Frank, N.; Edgerton, E. S.; Weber, R. J., Water-soluble organic aerosol material and the light-absorption characteristics of aqueous extracts measured over the southeastern United States. *Atmos. Chem. Phys.* 2010, 10, 5965-5977. doi:10.5194/acp-10-5965-2010
- 542 21. Noziere, B.; Dziedzic, P.; Cordova, A., Formation of secondary light-absorbing "fulvic-like" oligomers: a common process in aqueous and ionic atmospheric particles? *Geophys. Res. Lett.* **2007**, *34*, L21812. doi:10.1029/2007GL031300
- 545 22. Galloway, M. M.; Chhabra, P. S.; Chan, A. W. H.; Surratt, J. D.; Flagan, R. C.; Seinfeld, J. H.;
 546 Keutsch, F. N., Glyoxal uptake on ammonium sulphate seed aerosol: reaction products and
 547 reversibility of uptake under dark and irradiated conditions. *Atmos. Chem. Phys.* 2009, *9*, 3331 548 3345. doi:10.5194/acp-9-3331-2009
- Shapiro, E. L.; Szprengiel, J.; Sareen, N.; Jen, C. N.; Giordano, M. R.; McNeill, V. F., Light-absorbing secondary organic material formed by glyoxal in aqueous aerosol mimics. *Atmos. Chem. Phys.* 2009, *9*, 2289-2300. doi:10.5194/acp-9-2289-2009
- 24. Yasmeen, F.; Sauret, N.; Gal, J. F.; Maria, P. C.; Massi, L.; Maenhaut, W.; Claeys, M.,
 Characterization of oligomers from methylglyoxal under dark conditions: a pathway to
 produce secondary organic aerosol through cloud processing during nighttime. *Atmos. Chem. Phys.* 2010, 10, (8), 3803-3812. doi:10.5194/acp-10-3803-2010
- 556 25. Sareen, N.; Schwier, A. N.; Shapiro, E. L.; Mitroo, D.; McNeill, V. F., Secondary organic material formed by methylglyoxal in aqueous aerosol mimics. *Atmos. Chem. Phys.* **2010**, *10*, 997-1016. doi:10.5194/acp-10-997-2010
- 26. Hawkins, L. N.; Lemire, A. N.; Galloway, M. M.; Corrigan, A. L.; Turley, J. J.; Espelien, B.
 M.; De Haan, D. O., Maillard Chemistry in Clouds and Aqueous Aerosol As a Source of
 Atmospheric Humic-Like Substances. *Environ Sci Technol* 2016, 50, 7443-7452.
 doi:10.1021/acs.est.6b00909
- 27. Gao, Y.; Zhang, Y., Formation and photochemical investigation of brown carbon by hydroxyacetone reactions with glycine and ammonium sulfate. *RSC Adv.* **2018**, *8*, (37), 20719-20725. doi:10.1039/C8RA02019A

- 28. Hensley, J. C.; Birdsall, A. W.; Valtierra, G.; Cox, J. L.; Keutsch, F. N., Revisiting the reaction of dicarbonyls in aerosol proxy solutions containing ammonia: the case of butenedial. *Atmos. Chem. Phys.* 2021, *21*, (11), 8809-8821. doi:10.5194/acp-21-8809-2021
- 569 29. Noziere, B.; Cordova, A., A kinetic and mechanistic study of the amino acid catalyzed aldol condensation of acetaldehyde in aqueous and salt solutions. *J. Phys. Chem.* **2008**, *112*, (13), 2827-2837. doi:10.1021/jp7096845
- 30. Altieri, K. E.; Seitzinger, S. P.; Carlton, A. G.; Turpin, B. J.; Klein, G. C.; Marshall, A. G.,
 Oligomers formed through in-cloud methylglyoxal reactions: chemical composition,
 properties, and mechanisms investigated by ultra-high resolution FT-ICR mass spectrometry.
 Atmos. Environ. 2008, 42, 1476-1490. doi:10.1016/j.atmosenv.2007.11.015
- 31. Kampf, C. J.; Jakob, R.; Hoffmann, T., Identification and characterization of aging products in the glyoxal/ammonium sulfate system -- implications for light-absorbing material in atmospheric aerosols. *Atmos. Chem. Phys.* **2012**, *12*, 6323-6333. doi:10.5194/acp-12-6323-2012
- 32. Lin, P.; Laskin, J.; Nizkorodov, S. A.; Laskin, A., Revealing Brown Carbon Chromophores Produced in Reactions of Methylglyoxal with Ammonium Sulfate. *Environ Sci Technol* **2015**, 49, (24), 14257-14266. doi:10.1021/acs.est.5b03608
- 33. De Haan, D. O.; Hawkins, L. N.; Welsh, H. G.; Pednekar, R.; Casar, J. R.; Pennington, E. A.; de Loera, A.; Jimenez, N. G.; Symons, M. A.; Zauscher, M.; Pajunoja, A.; Caponi, L.; Cazaunau, M.; Formenti, P.; Gratien, A.; Pangui, E.; Doussin, J. F., Brown carbon production in ammonium- or amine-containing aerosol particles by reactive uptake of methylglyoxal and photolytic cloud cycling. *Environmental Science & Technology* **2017**, *in press*. doi:10.1021/acs.est.7b00159
- 34. Hawkins, L. N.; Welsh, H. G.; Alexander, M. V., Evidence for pyrazine-based chromophores
 in cloud water mimics containing methylglyoxal and ammonium sulfate. *Atmos. Chem. Phys.*2018, 18, (16), 12413-12431. doi:10.5194/acp-18-12413-2018
- 592 35. Chang, J. L.; Thompson, J. E., Characterization of colored products formed during irradiation 593 of solutions containing H₂O₂ and phenolic compounds. *Atmos. Environ.* **2010**, *44*, 541-551. 594 doi:10.1016/j.atmosenv.2009.10.042
- 36. Ofner, J.; Krüger, H. U.; Grothe, H.; Schmitt-Kopplin, P.; Whitmore, K.; Zetzsch, C., Physicochemical characterization of SOA derived from catechol and guaiacol a model substance for the aromatic fraction of atmospheric HULIS. *Atmos. Chem. Phys.* **2011**, *11*, (1), 1-15. doi:10.5194/acp-11-1-2011
- 37. Yu, L.; Smith, J.; Laskin, A.; Anastasio, C.; Laskin, J.; Zhang, Q., Chemical characterization of SOA formed from aqueous-phase reactions of phenols with the triplet excited state of carbonyl and hydroxyl radical. *Atmos. Chem. Phys.* **2014**, *14*, (24), 13801-13816, 16 pp. doi:10.5194/acp-14-13801-2014
- 38. Yu, L.; Smith, J.; Laskin, A.; George, K. M.; Anastasio, C.; Laskin, J.; Dillner, A. M.; Zhang, Q., Molecular transformations of phenolic SOA during photochemical aging in the aqueous phase: competition among oligomerization, functionalization, and fragmentation. *Atmos. Chem. Phys.* **2016**, *16*, (7), 4511-4527. doi:10.5194/acp-16-4511-2016
- 39. Smith, J. D.; Kinney, H.; Anastasio, C., Phenolic carbonyls undergo rapid aqueous photodegradation to form low-volatility, light-absorbing products. *Atmos. Environ.* **2016**, *126*, 36-44. doi:http://dx.doi.org/10.1016/j.atmosenv.2015.11.035

- 40. Xu, J.; Cui, T.; Fowler, B.; Fankhauser, A.; Yang, K.; Surratt, J. D.; McNeill, V. F., Aerosol
 Brown Carbon from Dark Reactions of Syringol in Aqueous Aerosol Mimics. *ACS Earth and Space Chemistry* 2018, 2, (6), 608-617. doi:10.1021/acsearthspacechem.8b00010
- 41. Vione, D.; Albinet, A.; Barsotti, F.; Mekic, M.; Jiang, B.; Minero, C.; Brigante, M.;
 Gligorovski, S., Formation of substances with humic-like fluorescence properties, upon photoinduced oligomerization of typical phenolic compounds emitted by biomass burning.
 Atmos. Environ. 2019, 206, 197-207. doi:https://doi.org/10.1016/j.atmosenv.2019.03.005
- 42. Lavi, A.; Lin, P.; Bhaduri, B.; Carmieli, R.; Laskin, A.; Rudich, Y., Characterization of Light Absorbing Oligomers from Reactions of Phenolic Compounds and Fe(III). ACS Earth and
 Space Chemistry 2017. doi:10.1021/acsearthspacechem.7b00099
- 43. Al Nimer, A.; Rocha, L.; Rahman, M. A.; Nizkorodov, S. A.; Al-Abadleh, H. A., Effect of
 Oxalate and Sulfate on Iron-Catalyzed Secondary Brown Carbon Formation. *Environ Sci Technol* 2019, *53*, (12), 6708-6717. doi:10.1021/acs.est.9b00237
- 44. Link, N.; Removski, N.; Yun, J.; Fleming, L. T.; Nizkorodov, S. A.; Bertram, A. K.; Al Abadleh, H. A., Dust-Catalyzed Oxidative Polymerization of Catechol and Its Impacts on Ice
 Nucleation Efficiency and Optical Properties. ACS Earth and Space Chemistry 2020.
 doi:10.1021/acsearthspacechem.0c00107
- 45. De Haan, D. O.; Hawkins, L. N.; Tolbert, M. A.; Doussin, J. F., Glyoxal's impact on dry ammonium salts: fast and reversible surface aerosol browning (Raw Data). *Chemistry and Biochemistry: Faculty Scholarship (Digital Repository)* **2020**, (40). doi:https://doi.org/10.22371/02.2020.006
- 46. Lee, H. J.; Aiona, P. K.; Laskin, A.; Laskin, J.; Nizkorodov, S. A., Effect of solar radiation on the optical properties and molecular composition of laboratory proxies of atmospheric brown carbon. *Environ. Sci. Technol.* **2014**, *48*, (17), 10217-10226. doi:10.1021/es502515r
- 47. Dasari, S.; Andersson, A.; Bikkina, S.; Holmstrand, H.; Budhavant, K.; Satheesh, S.; Asmi, E.;
 Kesti, J.; Backman, J.; Salam, A.; Bisht, D. S.; Tiwari, S.; Hameed, Z.; Gustafsson, Ö.,
 Photochemical degradation affects the light absorption of water-soluble brown carbon in the
 South Asian outflow. *Science Advances* 2019, 5, (1), eaau8066. doi:10.1126/sciadv.aau8066
- 48. O'Brien, R. E.; Kroll, J. H., Photolytic Aging of Secondary Organic Aerosol: Evidence for a
 Substantial Photo-Recalcitrant Fraction. *The Journal of Physical Chemistry Letters* 2019, *10*,
 (14), 4003-4009. doi:10.1021/acs.jpclett.9b01417
- 49. Browne, E. C.; Zhang, X.; Franklin, J. P.; Ridley, K. J.; Kirchstetter, T. W.; Wilson, K. R.;
 Cappa, C. D.; Kroll, J. H., Effect of heterogeneous oxidative aging on light absorption by
 biomass-burning organic aerosol. *Aerosol Sci. Technol.* 2019, 1-15.
 doi:10.1080/02786826.2019.1599321
- 50. Fleming, L. T.; Lin, P.; Roberts, J. M.; Selimovic, V.; Yokelson, R.; Laskin, J.; Laskin, A.;
 Nizkorodov, S. A., Molecular composition and photochemical lifetimes of brown carbon chromophores in biomass burning organic aerosol. *Atmos. Chem. Phys.* 2020, 20, (2), 1105-1129. doi:10.5194/acp-20-1105-2020
- 51. Jones, S. H.; Friederich, P.; Donaldson, D. J., Photochemical Aging of Levitated Aqueous
 Brown Carbon Droplets. ACS Earth and Space Chemistry 2021.
 doi:10.1021/acsearthspacechem.1c00005
- 52. Chen, L.-W. A.; Chow, J. C.; Wang, X.; Cao, J.; Mao, J.; Watson, J. G., Brownness of Organic
 Aerosol over the United States: Evidence for Seasonal Biomass Burning and Photobleaching
 Effects. *Environ Sci Technol* 2021. doi:10.1021/acs.est.0c08706

- 53. Rossignol, S.; Aregahegn, K. Z.; Tinel, L.; Fine, L.; Noziere, B.; George, C., Glyoxal Induced
 Atmospheric Photosensitized Chemistry Leading to Organic Aerosol Growth. *Environ. Sci. Technol.* 2014, 48, (6), 3218-3227. doi:10.1021/es405581g
- 658 54. Chen, Q.; Mu, Z.; Xu, L.; Wang, M.; Wang, J.; Shan, M.; Fan, X.; Song, J.; Wang, Y.; Lin, P.; 659 Du, L., Triplet-state organic matter in atmospheric aerosols: Formation characteristics and 660 Environ. potential effects on aerosol aging. Atmos. 2021, 252, 118343. 661 doi:https://doi.org/10.1016/j.atmosenv.2021.118343
- 55. Jiang, W.; Misovich, M. V.; Hettiyadura, A. P. S.; Laskin, A.; McFall, A. S.; Anastasio, C.;
 Zhang, Q., Photosensitized Reactions of a Phenolic Carbonyl from Wood Combustion in the
 Aqueous Phase—Chemical Evolution and Light Absorption Properties of AqSOA. *Environ Sci Technol* 2021. doi:10.1021/acs.est.0c07581
- 56. Zhao, R.; Lee, A. K. Y.; Abbatt, J. P. D., Investigation of Aqueous-Phase Photooxidation of Glyoxal and Methylglyoxal by Aerosol Chemical Ionization Mass Spectrometry: Observation of Hydroxyhydroperoxide Formation. *The Journal of Physical Chemistry A* 2012, *116*, (24), 6253-6263. doi:10.1021/jp211528d
- 57. Sareen, N.; Moussa, S. G.; McNeill, V. F., Photochemical Aging of Light-Absorbing Secondary Organic Aerosol Material. *The Journal of Physical Chemistry A* **2013**, *117*, (14), 2987-2996. doi:10.1021/jp309413j
- 58. Zhao, R.; Lee, A. K. Y.; Huang, L.; Li, X.; Yang, F.; Abbatt, J. P. D., Photochemical processing
 of aqueous atmospheric brown carbon. *Atmos. Chem. Phys.* 2015, *15*, (11), 6087-6100.
 doi:10.5194/acp-15-6087-2015
- 676 59. Aiona, P. K.; Lee, H. J.; Leslie, R.; Lin, P.; Laskin, A.; Laskin, J.; Nizkorodov, S. A., 677 Photochemistry of Products of the Aqueous Reaction of Methylglyoxal with Ammonium 678 Chemistry Sulfate. ACS Earth and Space 2017, 1, 522-532. (8),679 doi:10.1021/acsearthspacechem.7b00075
- 680 60. Vo, L.; Legaard, E.; Thrasher, C.; Jaffe, A.; Berden, G.; Martens, J.; Oomens, J.; O'Brien, R.
 681 E., UV/Vis and IRMPD Spectroscopic Analysis of the Absorption Properties of Methylglyoxal
 682 Brown Carbon. ACS Earth and Space Chemistry 2021, 5, (4), 910-919.
 683 doi:10.1021/acsearthspacechem.1c00022
- 684 61. Wong, J. P. S.; Nenes, A.; Weber, R. J., Changes in Light Absorptivity of Molecular Weight 685 Separated Brown Carbon Due to Photolytic Aging. *Environ Sci Technol* **2017**, *51*, (15), 8414-686 8421. doi:10.1021/acs.est.7b01739
- 687 62. He, Q.; Tomaz, S.; Li, C.; Zhu, M.; Meidan, D.; Riva, M.; Laskin, A.; Brown, S. S.; George,
 688 C.; Wang, X.; Rudich, Y., Optical Properties of Secondary Organic Aerosol Produced by
 Nitrate Radical Oxidation of Biogenic Volatile Organic Compounds. *Environ Sci Technol* 690 2021. doi:10.1021/acs.est.0c06838
- 691 63. Wang, J.; Doussin, J. F.; Perrier, S.; Perraudin, E.; Katrib, Y.; Pangui, E.; Picquet-Varrault, B.,
 692 Design of a new multi-phase experimental simulation chamber for atmospheric photosmog,
 693 aerosol and cloud chemistry research. *Atmos. Meas. Tech.* **2011**, *4*, 2465-2494.
 694 doi:10.5194/amt-4-2465-2011
- 695 64. De Haan, D. O.; Tapavicza, E.; Riva, M.; Cui, T.; Surratt, J.; Smith, A. C.; Jordan, M.-C.; Nilakantan, S.; Almodovar, M.; Stewart, T. N.; de Loera, A.; De Haan, A. C.; Cazaunau, M.;
- 697 Gratien, A.; Pangui, E.; Doussin, J. F., Nitrogen-containing, light-absorbing oligomers
- produced in aerosol particles exposed to methylglyoxal, photolysis, and cloud cycling. *Environ. Sci. Technol.* **2018,** *52*, (7), 4061-4071. doi:10.1021/acs.est.7b06105

- 65. Lin, P.; Fleming, L. T.; Nizkorodov, S. A.; Laskin, J.; Laskin, A., Comprehensive Molecular
 Characterization of Atmospheric Brown Carbon by High Resolution Mass Spectrometry with
 Electrospray and Atmospheric Pressure Photoionization. *Anal. Chem.* 2018, 90, (21), 12493 12502. doi:10.1021/acs.analchem.8b02177
- 66. Powelson, M. H.; Espelien, B. M.; Hawkins, L. N.; Galloway, M. M.; De Haan, D. O., Brown carbon formation by aqueous-phase aldehyde reactions with amines and ammonium sulfate. Environ Sci Technol **2014**, 48, (2), 985-993. doi:10.1021/es4038325
- 707 67. Trainic, M.; Riziq, A. A.; Lavi, A.; Rudich, Y., Role of interfacial water in the heterogeneous uptake of glyoxal by mixed glycine and ammonium sulfate aerosols. *Journal of Physical Chemistry A* **2012**, *116*, 5948-5957. doi:10.1021/jp2104837
- 68. Drozd, G. T.; McNeill, V. F., Organic matrix effects on the formation of light-absorbing compounds from [small alpha]-dicarbonyls in aqueous salt solution. *Environmental Science: Processes & Impacts* 2014, *16*, (4), 741-747. doi:10.1039/C3EM00579H
- 69. Gómez Alvarez, E.; Wortham, H.; Strekowski, R.; Zetzsch, C.; Gligorovski, S., Atmospheric
 Photosensitized Heterogeneous and Multiphase Reactions: From Outdoors to Indoors. *Environ* Sci Technol 2012, 46, (4), 1955-1963. doi:10.1021/es2019675
- 716 70. De Haan, D. O.; Hawkins, L. N.; Welsh, H. G.; Pednekar, R.; Casar, J. R.; Pennington, E. A.; 717 de Loera, A.; Jimenez, N. G.; Symons, M. A.; Zauscher, M.; Pajunoja, A.; Caponi, L.; 718 Cazaunau, M.; Formenti, P.; Gratien, A.; Pangui, E.; Doussin, J. F., Brown carbon production 719 in ammonium- or amine-containing aerosol particles by reactive uptake of methylglyoxal and 720 photolytic cloud cycling. Environ Sci Technol **2017**, 51, (13), 7458-7466. 721 doi:10.1021/acs.est.7b00159
- 71. Hensley, J. C.; Birdsall, A. W.; Keutsch, F. N., Competition of Partitioning and Reaction Controls Brown Carbon Formation from Butenedial in Particles. *Environ Sci Technol* **2021**, 55, (17), 11549-11556. doi:10.1021/acs.est.1c02891
- 72. Saleh, R., From Measurements to Models: Toward Accurate Representation of Brown Carbon in Climate Calculations. *Current Pollution Reports* **2020**, *6*, (2), 90-104. doi:10.1007/s40726-020-00139-3
- 73. Pospisilova, V.; Bell, D. M.; Lamkaddam, H.; Bertrand, A.; Wang, L.; Bhattu, D.; Zhou, X.;
 Dommen, J.; Prevot, A. S. H.; Baltensperger, U.; El Haddad, I.; Slowik, J. G.,
 Photodegradation of α-Pinene Secondary Organic Aerosol Dominated by Moderately Oxidized
 Molecules. *Environ Sci Technol* 2021. doi:10.1021/acs.est.0c06752
- 732 74. Klodt, A. L.; Zhang, K.; Olsen, M. W.; Fernandez, J. L.; Furche, F.; Nizkorodov, S. A., Effect 733 of Ammonium Salts on the Decarboxylation of Oxaloacetic Acid in Atmospheric Particles. 734 ACS Earth 5, 931-940. and Space Chemistry 2021, (4),735 doi:10.1021/acsearthspacechem.1c00025
- 75. Axson, J. L.; Takahashi, K.; De Haan, D. O.; Vaida, V., Gas-phase water-mediated equilibrium between methylglyoxal and its geminal diol. *P. Natl. Acad. Sci. USA* **2010**, *107*, (15), 6687-6692. doi:10.1073/pnas.0912121107
- 739 76. Kroll, J. A.; Hansen, A. S.; Møller, K. H.; Axson, J. L.; Kjaergaard, H. G.; Vaida, V., Ultraviolet Spectroscopy of the Gas Phase Hydration of Methylglyoxal. *ACS Earth and Space Chemistry* **2017**, *1*, (6), 345-352. doi:10.1021/acsearthspacechem.7b00054
- 77. Grace, D. N.; Sharp, J. R.; Holappa, R. E.; Lugos, E. N.; Sebold, M. B.; Griffith, D. R.; Hendrickson, H. P.; Galloway, M. M., Heterocyclic Product Formation in Aqueous Brown Carbon Systems. *ACS Earth and Space Chemistry* **2019**, *3*, (11), 2472-2481.
- doi:10.1021/acsearthspacechem.9b00235

- 78. Aregahegn, K. Z.; Noziere, B.; George, C., Organic aerosol formation photo-enhanced by the formation of secondary photosensitizers in aerosols. *Faraday Discuss.* **2013**, *165*, 123-134. doi:10.1039/c3fd00044c
- 79. Teich, M.; van Pinxteren, D.; Kecorius, S.; Wang, Z.; Herrmann, H., First quantification of imidazoles in ambient aerosol particles: Potential photosensitizers, brown carbon constituents, and hazardous components. *Environ Sci Technol* **2016**, *50*, 1166-1173. doi:10.1021/acs.est.5b05474
- 80. Zhu, Y.; Xiao, L.; Zhao, M.; Zhou, J.; Zhang, Q.; Wang, H.; Li, S.; Zhou, H.; Wu, J.; Tian, Y.,
 A Series of Imidazole Derivatives: Synthesis, Two-Photon Absorption, and Application for
 Bioimaging. *BioMed Research International* 2015, 2015, 965386. doi:10.1155/2015/965386
- 81. Frka, S.; Dautović, J.; Kozarac, Z.; Ćosović, B.; Hoffer, A.; Kiss, G., Surface-active substances
 in atmospheric aerosol: an electrochemical approach. *Tellus B: Chemical and Physical Meteorology* 2012, 64, (1), 18490. doi:10.3402/tellusb.v64i0.18490
- 759 82. Tan, Y.; Lim, Y. B.; Altieri, K. E.; Seitzinger, S. P.; Turpin, B. J., Mechanisms leading to oligomers and SOA through aqueous photooxidation: insights from OH radical oxidation of acetic acid and methylglyoxal. *Atmos. Chem. Phys.* **2012**, *12*, 801-813. doi:10.5194/acp-12-801-2012
- 763 83. Tan, Y.; Perri, M. J.; Seitzinger, S. P.; Turpin, B. J., Effects of precursor concentration and acidic sulfate in aqueous glyoxal OH radical oxidation and implications for secondary organic aerosol. *Environ. Sci. Technol.* **2009**, *43*, (21), 8105-8112. doi:10.1021/es901742f